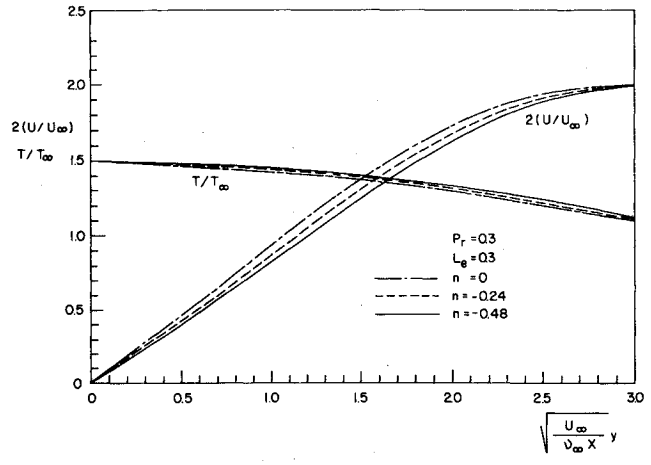

Fig. 3 Velocity and temperature dependence on n.

For an ideal gas, $n=-0.24$, in our solution we have used the following values: $n=0$ (identical to Liu[3]), $n=-0.24$ (the value appropriate for an ideal gas), and $n=-0.48$. Using this wide range of n enabled us to study the dependence of the solution upon it. Similarly, we have chosen two different values for Le (=0.3 and 0.15) and Pr (=0.3 and 0.65). Thus, the dependence of the flowfield on Le and Pr was also studied.

The temperature and velocity dependence on Pr and Le are shown in Figs. 1 and 2, respectively. While a change from 0.3 to 0.65 in Pr indicates a noticeable change in the profiles (Fig. 1), a change from 0.15 to 0.3 in Le hardly affects the velocity and temperature profiles.

Figure 3 illustrates the dependence of the flowfield on n. It is clearly seen that the smaller n is (i.e., more negative), the longer it takes to reach the inviscid uniform flow properties (i.e., the boundary layer is thicker).

Conclusions

The boundary-layer equations for a partially ionized frozen flow over a flat plate has been solved using a new approach in which the problem at hand was reduced from a two-point boundary value problem to a Cauchy problem, thus offering a simple, stable, and relatively inexpensive solution technique.

The method was applied to a strong shock-induced argon flow over an adiabatic flat plate. Since the method requires constant values for the Prandtl number, the Lewis number, and the exponential dependence n of the density viscosity product $\rho\mu$ upon the temperature T, the dependence of the flow inside the boundary layer on Pr, Le, and n was investigated. It was found that while Pr and n strongly affect the obtained flowfield, the influence of Le is negligibly small.

As a closing remark, it is of interest to note again that the findings of Liu et al.[4] indicate that the frozen behavior represents the shock-induced flowfield over a flat plate quite well and, hence, the frozen solution should not be considered as purely a sterile exercise.

References

[1] Schlichting, H., *Boundary Layer Theory*, McGraw-Hill Book Co., New York 1960.

[2] Stewartson, K., "The Theory of Laminar Boundary Layers in Compressible Fluids," Oxford Mathematical Monographs, Oxford University Press, Oxford, England, 1964.

[3] Liu, W. S., "The Analysis of Shock Structure and Nonequilibrium Boundary-Layer Induced by a Normal Shock Wave in an Ionized Argon Flow," UTIAS Report No. 198, Univ. of Toronto, Toronto, Ontario, Canada, 1975.

[4] Liu, W. S., Whitten, B. T., and Glass, I. I., "Ionizing Argon Boundary Layer. Part 1. Quasi-Steady Flat-Plate Laminary Boundary-Layer Flows," *Journal of Fluid Mechanics*, Vol. 87, Pt. 4, 1978, pp. 609-640.

[5] Yaknot, A., Ben-Dor, G., Rakib, Z., and Igra, O., "A New Approach to the Solution of the Boundary Layer Equations of an Ideal Compressible Flow over a Flat Plate," *Aeronautical Journal*, Paper No. 845, Jan. 1981, pp. 34-35.

[6] Ben-Dor, G., Rakib, Z., and Igra, O., "The Boundary Layer of a Compressible Singly Ionized Frozen Flow over a Flat Plate-A New Method of Solution," Collection of Papers of the 25th Israel Annual Conference on Aviation and Astronautics, 1983.

[7] Töpfer, C., "Bemerkungen zu dem Aufsatz von H. Blasius," *Zeitschr. f. Math. a Phys.*, Vol 60, 1912, pp. 397-398.

[8] Ben-Dor, G. Rakib, Z., and Igra, O., "Frozen-Plasma Boundary-Layer Flows over Isothermal Flat Plates-Parametric Study," *AIAA Journal*, Vol. 22, Feb. 1984, pp. 299-301.

Shock Shape over a Sphere Cone in Hypersonic High Enthalpy Flow

S.L. Gai,* R.J. Sandeman,† P. Lyons,‡ and D. Kilpin§
The Australian National University, Canberra, Australia

Introduction

THE flowfield of a blunt-nosed body in hypersonic/hypervelocity flight has many complex features. These include subsonic flow in the stagnation region, flow rotationality, and, in addition, nonequilibrium phenomena such as dissociation and recombination. Under these circumstances, the mechanisms which influence pressures and heat-transfer rates on the surface of the body are the result of complex interaction of compression and expansion waves which originate due to body shape, reflection of waves from shock surface and sonic line, and wave reflections from the vorticity layer near the surface due to nonequilibrium flow.

As shown by Traugott,[1] this complex interaction is due, in part, to the transition that the flow has to make from the nose to the afterbody. In particular, at hypersonic Mach numbers, depending on whether the afterbody is slender (e.g., a hemisphere cylinder) or nonslender (e.g., blunted cone at an incidence), the flow may undergo either underexpansion or overexpansion. This would then cause marked deviations from thermodynamic equilibrium as theorized by Bloom and Steiger,[2] and confirmed by present results.

Flow Features

The overexpansion in the vicinity of transition leads to some pressure rise immediately following the expansion which is due to two reasons. Firstly, as a result of expansion and consequent thinning of the boundary layer in the shoulder region, the streamlines curve inward near the surface. This is evidenced by the interferometric observations of Giese and Bergdolt[3] on the flow over a truncated cone. Second, the curvature of streamlines gives rise to expansion waves which reflect back from the sonic line as well as from the bow shock as compression waves, which will then reinforce the afterbody (cone) shock thus giving rise to an inflection in the shock

Received Feb. 11, 1983; revision received Sept. 9, 1983.

*Research Fellow, Department of Physics; presently, Dept. of Mechanical Engineering, University of New South Wales, Royal Military College, Duntroon, Australia. Member AIAA.
†Reader, Department of Physics.
‡Research Assistant, Department of Physics.
§Visiting Fellow, Department of Physics.

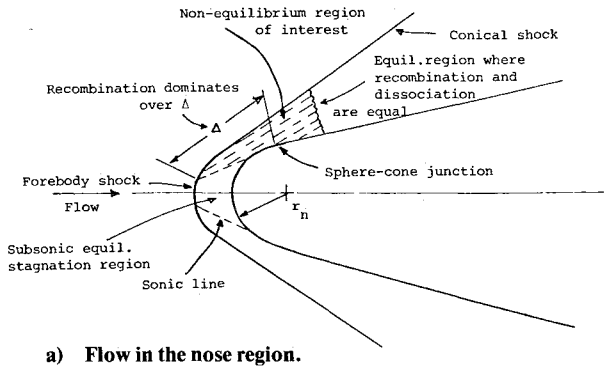

a) Flow in the nose region.

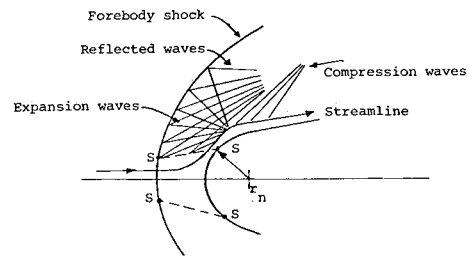

b) Flow within the transition (Δ) region (scale exaggerated).

Fig. 1 Flow schematics.

surface (see Fig. 1). This inflection in the shock curvature would be slightly aft of the sphere-cone junction and its position would vary with the (effective) cone angle and Mach number. The existence of shock inflection points is thus, at least in part, connected with the associated pressure distribution and the curvature of streamlines. On the other hand, for an underexpanded type of pressure distribution no shock inflection point is to be expected.[1]

While Traugott[1] does not provide experimental evidence of shock inflection point, Nagamatsu et al.[4] have observed such an inflection point on the shock wave in their experiments on flow over blunt bodies in hypersonic high enthalpy streams. The authors have not encountered any other evidence.¶

It is well known that nonequilibrium effects influence shock curvature.[5,6] Expressed simply, the relation between the streamline and shock curvature is

$$K_s = F_1 K_w + F_2 \left[\frac{1}{r} + \frac{f_1}{\sin\theta} \right]$$

where K_w and K_s are shock and streamline curvatures and F_1, F_2, f_1, and θ are constants depending on geometry and freestream conditons. F_1, F_2, f_1, and θ have the same meaning as in Ref. 6. To obtain K_w one has to specify the values of K_s, r, and the steamline inclination θ. For the range of present experiments, the values of F_1, F_2, and f_1 are of the order of 2, 4×10^{-2} and -10^{-2}, respectively.

Considering the bracketed term in the preceding equation, we note that in the shock layer the nonequilibrium effects would predominate away from the surface, whereas vorticity effects dominate the surface vicinity. This is consistent with the observation of Sedney and Gerber[7] that entropy effects are concentrated near the surface, while near the shock relaxation effects predominate. Sedney and Gerber also predict considerable overexpansion as a result of flow nonequilibrium and axisymmetry. They do not, however, discuss shock and streamline curvatures due to such an overexpansion.

¶While Giese and Bergdolt's interferograms[3] suggest the existence of an inflection point, it is due mainly to secondary shock from boundary-layer separation around the truncated corner intersecting the main cone shock.

Experiments and Discussion of Results

Tests on a spherical nose cone of a total angle of 26 deg at various angles of incidence were conducted in the Australian National University free-piston shock tunnel T3 (Ref. 8) with nitrogen as the test gas. The flow was generated by a conical nozzle whose exit and throat diameters were 203 and 12.7 mm, respectively. The freestream was a dissociated nitrogen (the dissociation fraction c_l varying from 0.01 to 0.5) at speeds (U_∞) ranging from 5 to 8 km s^{-1} and a Mach number of approximately 6. The corresponding reservoir enthalpies (h_0) ranged from 15 to 50 MJ/kg, respectively.

The freestream conditions were calculated at the exit plane of the nozzle using a computer program based on the method of Lordi et al.[9] for nonequilibrium gas expansions.

Self-luminosity photographs, taken with a fast electromechanical shutter speed ($\simeq$800 cm s^{-1}) especially developed for these experiments,[10] were used to study shock shapes. Some of these photographs are shown in Fig. 2.

The photographs show that an inflection point on the shock wave appears immediately downstream of the sphere-cone junction on the windward side when the angle of attack is greater than about 6 deg (or effective angle of attack of the cone is approximately 19 deg). The inflection point becomes more perceptible and moves upstream as the angle of attack is increased. This is evident from the photographs of $\alpha = 12$ and 20 deg. It is also interesting to note that with increasing enthalpy, the cone shock moves closer to the surface. Such an observation also has been made by Nagamatsu et al.,[4] who attribute this to nonequilibrium gas effects. Closer examination of their measurements also shows strong overexpansion effects. Our results confirm these observations. Further, while Nagamatsu et al.[4] found that the inflection point became less perceptible at higher stagnation temperatures (i.e., higher enthalpy), the present results do not give such an indication even though the stagnation temperatures (T_0) varied from 8,000 to 12,000 K. In order to study this phenomena further, some experiments were conducted with argon to observe the perfect gas behavior. These experiments showed that the shock inflection and strong overexpansion present in the dissociated nitrogen flow did not appear. This would suggest that the strong shock inflection observed with nitrogen is the result of flow nonequilibrium.

Bloom and Steiger[2] suggest that for the flow in the shoulder region, a simple Prandtl-Meyer type expansion may be assumed to start from the sonic line which is located slightly upstream of the sphere-cone junction. The flow in the stagnation region is assumed to be in equilibrium (see Fig. 1). The diatomic nitrogen which is dissociated into atoms may now recombine into molecules as a result of three body collisions in the expansion region whose length scale is $\Delta = 0(r_n)$ where r_n is the spherical nose radius.

Assuming the gas to be in recombination-dominated chemical nonequilibrium and neglecting temperature dependence effect,

$$\dot{W} < 0 \quad \text{and} \quad \dot{W}/\rho \sim p^2$$

where $\dot{W}$ is the net rate of atomic mass production by chemical reaction and p is the surface pressure.[11]

Using the data of Ref. 12 on dissociated nitrogen flow over blunt bodies and the recombination rate parameter for nitrogen,[2] the dissociation fraction falls by about 20-30% over Δ for the present experimental conditions, thus showing pronounced nonequilibrium gas effects in this region.

In conclusion, for the type of blunt body studied, nonequilibrium effects upon the flowfield appear to be appreciable, particularly on the shock wave, which tends to move closer to the body with increasing enthalpy showing an inflection point. Existence of such an inflection point is also not ruled out by theory.[13] Further experiments on this problem are in progress.

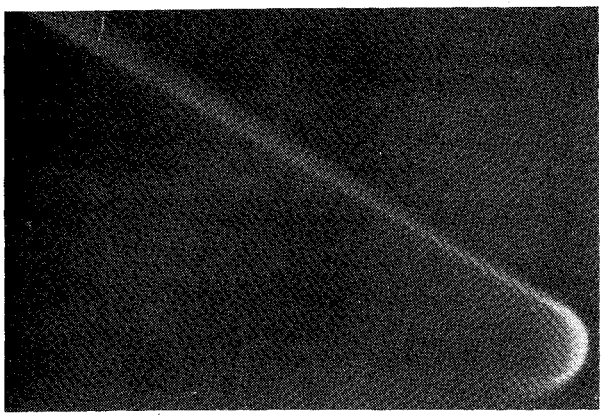

a) h_0(MJ/kg) = 30; U_0(km/s) = 6; α = 6.

b) h_0(MJ/kg) = 30; U_0(km/s) = 6; α = 12.

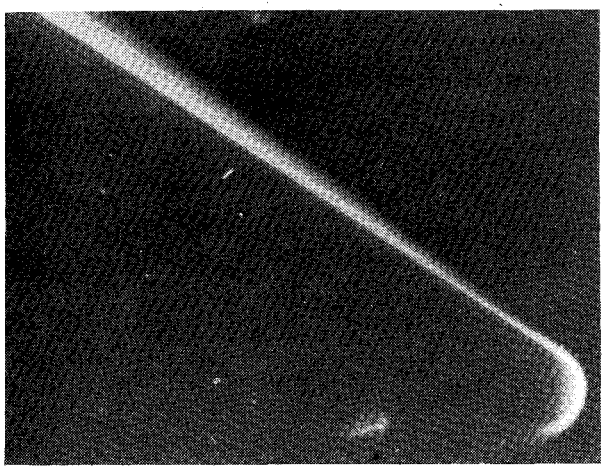

c) h_0(MJ/kg) = 52; U_0(km/s) = 8; α = 12.

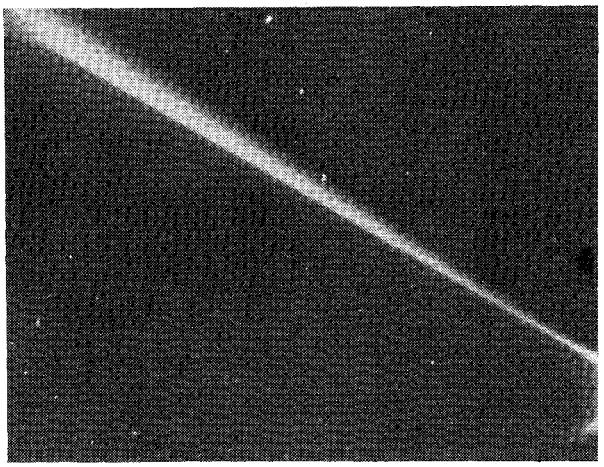

d) h_0(MJ/kg) = 30; U_0(km/s) = 6; α = 15.

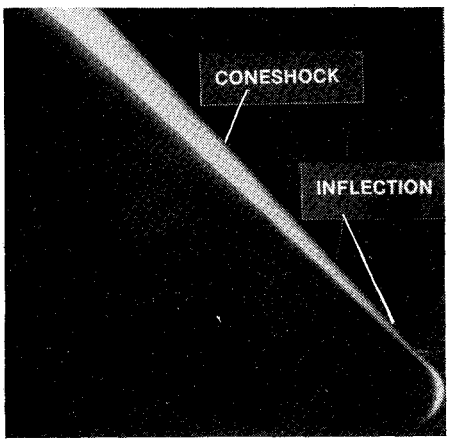

e) h_0(MJ/kg) = 52; U_0(km/s) = 8; α = 20.

Fig. 2 Sphere-cone body shocks in nitrogen.

Acknowledgments

The authors would like to thank V. Adams and K. Smith for technical and photographic assistance. This work was supported by a grant from the Australian Research Grants Scheme.

References

[1] Traugott, S.C., "Some Features of Supersonic and Hypersonic Flow about Blunted Cones," *Journal of the Aerospace Sciences,* Vol. 29, April 1962, pp. 389-399.

[2] Bloom, M.H. and Steiger, M.H., "Inviscid Flow with Nonequilibrium Molecular Dissociation for Pressure Distributions Encountered in Hypersonic Flight," *Journal of the Aerospace Sciences,* Vol. 27, Nov. 1960, pp. 821-840.

[3] Giese, J.H. and Bergdolt, V.E., "Interferometric Studies of Supersonic Flows about Truncated Cones," *Journal of Applied Physics,* Vol. 24, Nov. 1953, pp. 1389-1396.

[4] Nagamatsu, H.T., Geiger, R.E., and Sheer, R.E., "Real Gas Effects in Flow over Blunt Bodies at Hypersonic Speeds," *Journal of the Aerospace Sciences,* Vol. 27, April 1960, pp. 241-251.

[5] Sedney, R., "Some Aspects of Nonequilibrium Flows," *Journal of the Aerospace Sciences,* Vol. 28, March 1961, pp. 189-208.

[6] Hsu, C.T., "On the Gradient Functions for Nonequilibrium Dissociative Flow Behind a Shock," *Journal of the Aerospace Sciences,* Vol. 28, April 1961, pp. 337-339.

[7] Sedney, R. and Gerber, N., "Nonequilibrium Flow over a Cone," *AIAA Journal,* Vol. 1, Nov. 1963, pp. 2482-2486.

[8] Stalker, R.J., "Development of a Hypervelocity Wind Tunnel," *The Aeronautical Journal, Royal Aeronautical Society,* Vol. 76, June 1972, pp. 374-384.

[9]Lordi, J.A., Mates, R.E., and Moselle, J.R., "Computer Program for the Numerical Solution of Nonequilibrium Expansions of Reacting Gas Mixtures," NASA CR-472, 1966.
[10]Lyons, P., Kilpin, D., and Gai, S.L., "A New High Speed Electro-Mechanical Shutter," *Journal of Scientific Instruments,* Vol. 17, Jan. 1984, pp. 108-109.
[11]Inger, G.R., "Nonequilibrium Dissociated Boundary Layers with a Reacting-Inviscid Flow," *AIAA Journal,* Vol 1, Sept. 1963, pp. 2057-2061.
[12]Hornung, H.G., "Nonequilibrium Dissociating Nitrogen Flow over Spheres and Cylinders," *Journal of Fluid Mechanics,* Vol. 53, Pt. 1, 1972, pp. 149-176.
[13]Vincenti, W.G. and Kruger, C.H., *Introduction to Physical Gas Dynamics,* John Wiley and Sons, Inc., New York, 1965, p. 305.

Application of Riemann Problem Solvers to Wave Machine Design

Shmuel Eidelman*
Naval Postgraduate School, Monterey, California
Atul Mathur†
Exotech, Inc. Campbell, California
and
Raymond Shreeve‡ and Jack Erwin§
Naval Postgraduate School, Monterey, California

Nomenclature

p	= pressure, N/m^2
ρ	= density, kg/m^3
u	= velocity, m/s
x	= space coordinate (along rotor passage)
t	= time coordinate
H. P.	= high pressure
L. P.	= low pressure
[L]	= left
[R]	= right

Subscripts

1, 2, 3 ..., 10 = states shown in Fig. 1

The terms tubes, passages, and cells have been used interchangeably in the text.

Introduction

WAVE rotors are devices in which wave propagation is used to effect a transfer of energy between a gas and a rotating shaft or directly between one gas and another. Reviews of such devices and their general operating principles have been published[1,2] and their commercial applications have been developed.[3]

In the case of direct transfer of energy, one gas (driver) at high pressure is used to compress a second gas (driven). The process is arranged to occur in tube-like passages arranged on the periphery of a drum or rotor. The compression is achieved by means of compression waves or shock waves and the compressed gas is drawn off from the end of the tube in which the process takes place. The driver gas then undergoes a series of expansions to a lower pressure and is scavenged out by freshly inducted driven gas at approximately the same pressure level. This fresh "charge" is then compressed by the high pressure driver gas and the cycle repeats itself.

Steady rotation of the drum sequences the passage of the ends of the tubes past stationary inlet ports, outlet ports, and endwalls. This establishes unsteady but repetitive flow processes within the rotating tubes and essentially steady flow in the inlet and outlet ports.

Complicated unsteady wave phenomena appear in the working of these devices, and design of even the most simple mode of operation requires calculation of an array of wave processes such as shock waves, reflected and "hammer" shock waves (from a wall or moving interface), rarefaction waves (connecting two states of a gas or produced by tube end closure), as well as interactions between incident and reflected waves. In general, the two gases in these devices have considerably different ethalpies, leading to the formation of contact surfaces that also interact with the various waves. The flow in each tube is usually analyzed using one-dimensional or quasi-one-dimensional approaches, implying that changes in state occur only along the passage. This enables the wave processes to be depicted on an x-t plane. Such wave diagrams are extremely useful in the examination of possible wave cycles, providing visual information of the wave paths, proper placing of the ports, seeing interactions, and whether a particular cycle, "closes," the latter being necessary for cyclic operation. The construction of wave diagrams is usually quite involved, requiring considerable time and effort, since a mismatch in any one parameter gives rise to a new pressure wave which has to be accounted for through the complete rotational cycle. The method of characteristics, despite its limitations (only weak shocks are permitted), has been the technique generally used for carrying out cycle computations.[1] However, graphical methods of constructing wave diagrams are time consuming and may require weeks of tedious calculations.[4] Clearly, a fast and "user friendly" computational procedure is required to carry out preliminary design calculations for wave rotor devices.

The method described below offers a unified approach to the calculation of wave rotor cycles with no restriction on the strength of the waves involved.

The method has been exercised in the design of a wave-turbine experiment at the Naval Postgraduate School's

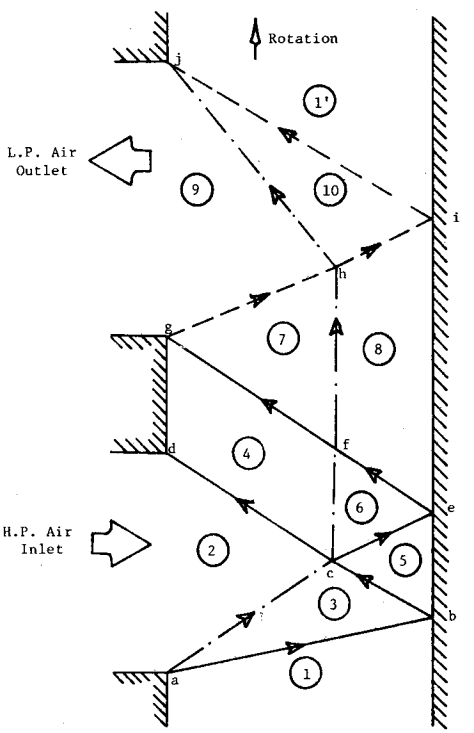

Fig. 1 Simplified wave diagram for "impulse turbine mode" operation.

Received Oct. 12, 1982. This paper is declared a work of the U. S. Government and therefore is in the public domain.
*NRC Research Associate.
†Project Engineer.
‡Program Director, Turbopropulsion Laboratory.
§Late NAVAIR Visiting Research Professor.